11. ECR Ion Sources

Daniela Leitner and Claude Lyneis

11.1 Introduction

ECR (Electron Cyclotron Resonance) ion sources are widely used for the production of high quality multiply charged ion beams for accelerators, atomic physics research and industrial applications. A wide variety of designs have evolved, tailored to their applications. The development and refinement of ECR ion sources over the last three decades has provided remarkable improvements in their performance. For example in 1980, Micromafios produced 15 eμA of O^{6+} [1] and 16 years later in 1996 the CAPRICE source produced 1100 eμA [2], an increase by a factor of 73! Recently the RIKEN 18 GHz source produced 2000 eμA of Ar^{8+} [3]. Development efforts for even more powerful ECR ion sources are underway, made possible by technical progress on magnets and microwave generators, which allows the application of stronger magnetic fields and higher frequencies. Research in nuclear physics with heavy ions continues to drive and fund the development of these sources to achieve higher charge state ions, and more intense beams with better emittance. The growing field of radioactive beam nuclear physics has added new impetus for the development a new generation of high frequency, high magnetic field ECR ion sources and for sources with high ionization efficiency for the production of beams from rare and or radioactive isotopes [4-6]. Recently, ECR ion sources have been developed to produce very high currents (>100 mA) of singly charged ions for accelerators [7].

Several general characteristics of ECR sources explain their widespread application in the accelerator community. Most important is the ability to produce CW beams from any element at useful intensities for nuclear and atomic physics research. Another characteristic of ECR sources is that the discharge is produced without cathodes. Therefore, only the source material injected into an ECR source is consumed. As a result, ECR sources can be operated continuously for long periods without interruption. Maintenance required on ECR sources is also minimal, consisting mainly of occasional repair of vacuum equipment, external ovens and electrical support equipment.

11.2 Brief History of the Development of ECR Ion Sources

The field of ECR ion sources has its roots in the plasma fusion developments in the late 1960's. The use of Electron Cyclotron Resonance Heating (ECRH) in plasma devices to produce high charge state ions was suggested in 1969 [8]. The first sources actually using ECRH to produce multiply charged ions were reported in 1972 in France by Geller et al [9] and in Germany by Wiesemann et al. [10]. These devices, which used solenoid magnetic mirror configurations and operated at pressures of 10^{-4} to 10^{-5} Torr, were capable of producing plasma densities of order 1×10^{12} cm^{-3} and keV electrons. However, the ion

confinement times were 10^{-4} s or less and this resulted in low charge state distributions (CSD) which, for example, peaked at N^{2+} for nitrogen and Ar^{2+} for argon.

A breakthrough occurred in 1974 when Geller and coworkers transformed a large mirror device used for plasma research (CIRCE) [11] into an extremely successful ion source, SUPERMAFIOS [12], which is shown in Figure 11.1. Unlike the earlier ion sources using ECRH, the magnetic field of CIRCE, renamed SUPERMAFIOS, used a hexapole field in addition to the solenoidal mirror field. This produced a minimum-B magnetic field configuration that stabilized the plasma against MHD instabilities. It also provided a closed ellipsoidal surface (the resonant zone) inside the plasma chamber where the electrons were heated by ECRH. With this configuration, the loss rate of hot electrons and of ions from the plasma was significantly reduced. In addition, CIRCE was a two-stage device. A cold plasma was generated in the first stage, operating at a higher pressure of about 10^{-3} Torr. This cold plasma flowed along the magnetic field lines, feeding the main confinement stage, which operated at much lower pressure, about 10^{-6} Torr. These new features, plasma stabilization in a minimum-B field configuration, a closed ECR surface, and a main stage operating at low neutral pressure, resulted in an enormous improvement in the lifetime of the ions in the source (~10^{-2} s) and shifted the CSD to much higher charge states. Several variations of this ECR source were tested between 1974 and 1977, however the basic features of the main stage design remained unchanged. The magnetic topology and axial extraction system associated with the main stage of SUPERMAFIOS are found in all modern high charge state ECR ion sources.

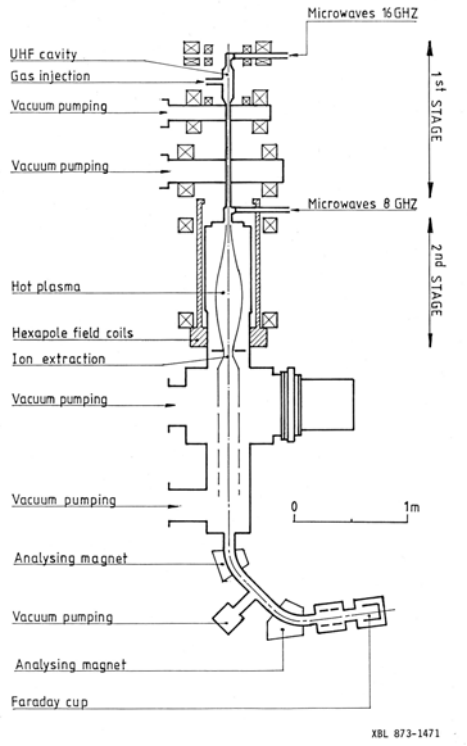

Figure 11.1: Schematic drawing of the SUPERMAFIOS ECR ion source (Courtesy of the Lawrence Berkeley National Laboratory)

The main drawback of SUPERMAFIOS was the 3 MW power consumed by the large room temperature copper coils needed to produce the solenoid and sextupole fields in the main stage. Different solutions were considered to reduce this power. The use of samarium-cobalt (Sm-Co) permanent magnets was initially considered impractical because it was assumed that ECR sources should be as large as SUPERMAFIOS (diameter 30 cm, length 100 cm). Therefore, projects to build large superconducting ECR sources were started in Louvain-la-Neuve [13], Karlsruhe [14] and Jülich [15].

In 1979 Geller transformed a reduced scale permanent magnet model hexapole built in Louvain-la-Neuve into a successful source of much smaller size (diameter 7 cm, length 30 cm) called MICROMAFIOS [1]. After development and modification it was renamed MINIMAFIOS [16]. MINIMAFIOS sources have since been built by Geller's group for laboratories at KVI-Groningen, SARA-Grenoble, GANIL-Caen, GSI/CERN-Geneva, and NAC-South Africa. In the period from 1980 to 1985, the development of ECR ion sources spread to other laboratories [17-22].

A second generation of ECR ion sources was launched in 1984 when the Grenoble group constructed a new source, MINIMAFIOS-16GHz, using higher microwave frequencies and stronger magnetic fields [23]. These improvements significantly increased both the total extracted current and the charge state distribution. Many second-generation ECR ion sources followed that also used higher frequencies and stronger magnetic fields to increase performance (see references in Table 11.1). While most of the sources used permanent magnets for the sextupole and copper coils for the solenoids, a number of fully superconducting ECR ion sources were built [24-26]. Recently, with advances in superconducting magnet technology, a new generation of high field superconducting sources is beginning to emerge, the first one being the superconducting source SERSE. The most advanced superconducting source now in operation is the VENUS ECR ion source, which is briefly described later in this chapter. However, several projects and design have been started around the world to build third generation superconducting ECR ion sources [27-31]

11.3 The LBNL ECR Ion Sources

In this section we describe two sources, the Advanced Electron Cyclotron Resonance-Upgrade (AECR-U) [32] and the Versatile ECR ion source for NUclear Science (VENUS) [29, 31], as examples of second and third generation ECR ion sources. To give the reader some perspective the performances of the two LBNL sources are compared with other high performance sources for selected beams in Table 11.1. In addition, SuperNanogan, a high performance, compact, fully permanent magnet ECR ion sources, is listed for comparison with the conventional 14 GHz ECR ion sources. Furthermore, the SERSE results at 28 GHz for Xe are also listed in Table 11.1 as a demonstration of the frequency scaling [33].

11.3.1 The AECR-U Ion Source

The AECR-U ion source is a conventional ECR ion source that has been optimized for the production of high charge state ions. The design combines all of the current ECR ion source improvement techniques. Shown in Figure 11.2 is a cross-sectional view of the AECR-U ion source. It was built in 1990 and was upgraded in 1996 to further enhance its performance. Slightly modified versions of this source are in operation at three other laboratories [34-36].

Table 11.1: Performance of various 14 and 18 GHz ECR ion sources. *Performance date for three frequency (8.6+10+14 GHz) operation have been taken from references [2, 37-39]

		SNanogan	*AECR-U*	*Caprice*	*GTS*	*RIKEN*	*SERSE*	*SERSE*	*VENUS*
f(GHz)		*14*	*10+14*	*14*	*18*	*18*	*14+18*	*28*	*18*
^{16}O	6^+	150	840*	1000	1500	1000	540		1100
	7^+	20	360*	190			225		324
^{40}Ar	8^+	330		800		1900			
	9^+	130		500		1000			
	11^+	70	270	200	405	300	260		290
	12^+	24	192	100			200		180
	13^+	8	120	40			130		
	14^+	1	82	15			84		
	16^+		25.6	1			21		
	17^+		3.1		1.8		2.6		
	18^+		0.25				0.4		
Xe	20^+			80	216	295	135	300	164
	25^+	6.5	46	40				216	
	26^+		46	40					
	27^+		30	20	92		78		84
	28^+		26.5	10	65				
	29^+		21	4					
	30^+		12		28	11	38.5	100	28
	31^+		7		18		23.5		15
	32^+	0.3	4.6			4	*		9
	33^+		2.9		7		9.1		3
	34^+		*				5.2	35	
	35^+		1.6						
	36^+		1				2		
	37^+		0.6						
	38^+		0.25					8	

Its maximum peak fields on axis are 1.7 and 1.1 Tesla at the injection and extraction regions, respectively. The axial fields are produced by hollow core copper coils with two iron yokes that enhance the field at injection and extraction while reducing it at the center. The maximum radial field at the inner surface of the aluminum plasma chamber is 0.85 Tesla, which is produced by a 12 piece NdFe-B sextupole. The aluminum plasma chamber is 30 cm in length with an inner diameter of 7.6 cm. Six radial slots and an external turbo pump give about 150 l/s pumping speed. The radial slots also provide easy oven access to the plasma chamber. The AECR-U plasma is driven by microwaves at two frequencies (14 and 10 GHz) launched through two of the three off-axis waveguides terminated at a bias plate in the injection region. Gas is bled into the source through one of the off-axis waveguides. Although its magnetic field strength is only about 60% of the highest field strength ECR ion sources in operation, the AECR-U is one of the highest performing 14 GHz ECR ion sources, especially for very high charge states. For example, a low intensity U^{64+} beam was produced with the AECR-U ion source and accelerated by the 88-Inch Cyclotron to 2.06 GeV [32].

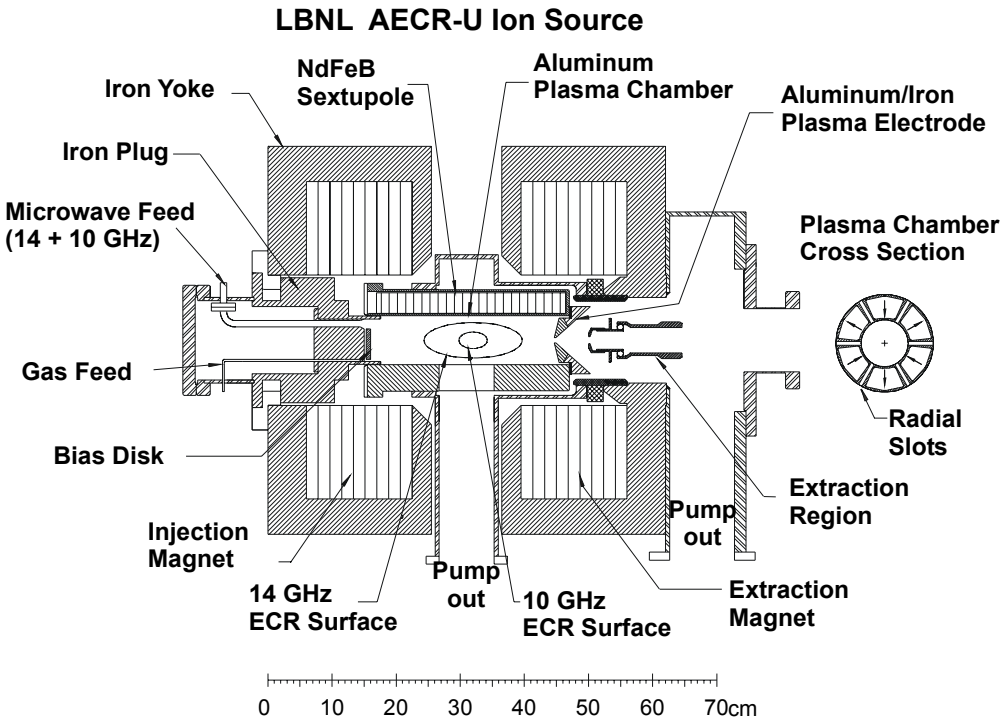

Figure 11.2: An elevation view of the AECR-U. The ECR zones for 10 and 14 GHz are indicated by ellipses at the center of the plasma chamber, since the source can be operated with two-frequency heating

11.3.2 The VENUS ECR Ion Source

VENUS is a third generation superconducting ECR ion source designed to produce high current, high charge state ions for the 88-Inch Cyclotron at the Lawrence Berkeley National Laboratory [29, 31, 40]. VENUS also serves as the prototype ion source for the RIA (Rare Isotope Accelerator) front end. The magnetic confinement configuration consists of three superconducting axial coils and six superconducting radial coils in a sextupole configuration. The nominal design fields of the axial magnets are 4 T at injection and 3 T at extraction; the nominal radial design field strength at the plasma chamber wall is 2 T, making VENUS the first ECR ion source to have optimum magnetic fields for 28 GHz operation.

This frequency choice has several design consequences. To achieve the required magnetic confinement, superconducting magnets have to be used. The size of the superconducting magnet structure implies a relatively large plasma volume. Consequently, high power 28 GHz microwave coupling becomes necessary to achieve sufficient plasma heating power densities. Finally, the extraction of the high current, multi-species ion beam from the ion source plasma in the presence of a high magnetic field is a challenging task, and VENUS will provide an essential database for the design of future ECR high current accelerator injector systems.

Figure 11.3.2 shows the mechanical layout of the ECR ion source. The mechanical design is described in detail elsewhere [29]. The water-cooling of the ion source is sufficient to allow continuous operation at 15 kW microwave input power.

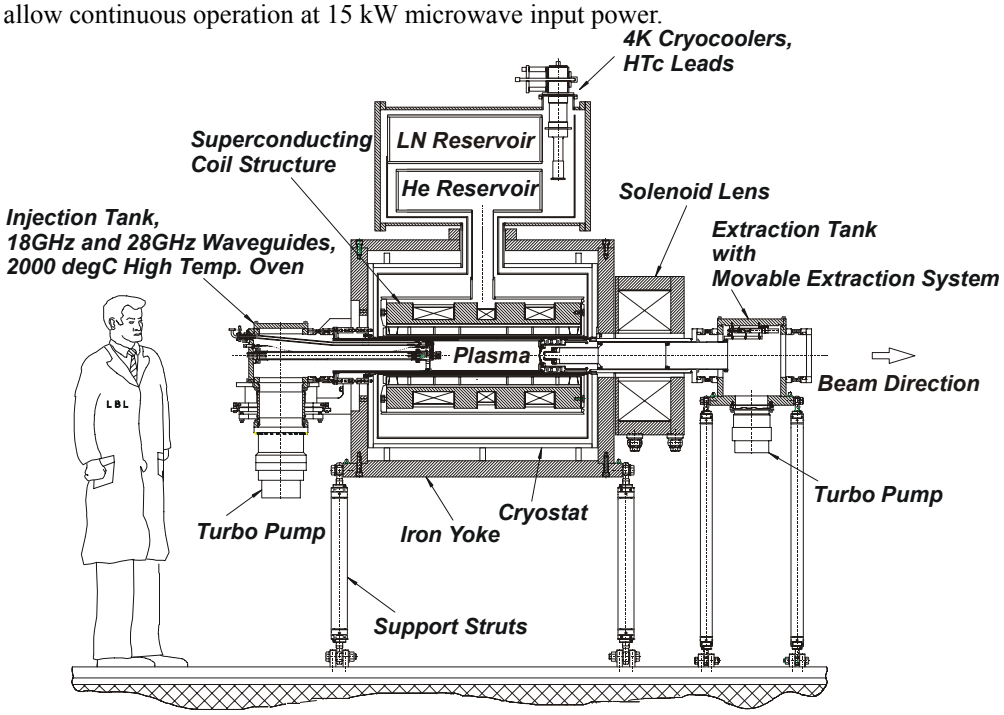

Figure 11.3: Mechanical layout of the VENUS ion source and cryogenic system

The design and development of the superconducting magnets are described in [41, 42]. The sextupole coils are wound around a core with iron in the center, which enhances the peak field about 10%. The superconducting sextupole coils experience strong forces in the axial field of the solenoids. Therefore, a new clamping scheme utilizing liquid metal filled bladders was developed to prevent any movement of the energized coils [42]. During commissioning of the superconducting magnets, the sextupole reached 110% of its design field after a few training quenches (2.4 T) with the solenoids operating at their design fields, 4 T at injection and 3 T at extraction respectively.

The cryogenic system for VENUS has been designed to operate at 4.2º K with two cryocoolers each providing up to 45 W of cooling power at 50º K and 1.5 W at 4º K in a closed loop mode without further helium transfer. The two cryocoolers provide sufficient cooling power for 18 GHz operation [40]. For 28 GHz operation, the expected X-ray flux will add to the heat load of the cryostat. Therefore, we are currently constructing a cryostat extension with an additional (third) cryocooler.

During 2003 VENUS was commissioned at 18 GHz and preparations for 28 GHz operation were started. Tests with various gases and metals were performed with up to 2000 W of 18 GHz RF power. Promising performance was measured in these preliminary beam tests. For example, 180 pμA of O^{6+}, 15 pμA of Ar^{12+}, 7.5 pμA of Xe^{20+} and 6.8 pμA of Bi^{24+}

were produced in the early commissioning phase. In FY04 a 10 kW, 28 GHz gyrotron system will be added, which will enable VENUS to reach full performance. A similar 28 GHz gyrotron system was used successfully for the first time in Catania in 2000 to power the SERSE ECR ion source [33]. The waveguide system planned for VENUS takes advantage of this development. The components are expected to be delivered in December of 2003 and commissioning of VENUS at 28 GHz will begin in the Spring of 2004.

11.4 Physics and Operation of ECR Ion Sources

ECR ion sources use magnetic confinement and electron cyclotron resonance heating to produce a plasma made up of energetic electrons and relatively cold ions. The plasma electrons have two components, a cold population (~20 eV) and a hot population that has a high energy tail reaching up to 100 keV or more. Typical ion energies are a few eV. The electrons produce the high charge state ions primarily by sequential impact ionization. The ions and the electrons must be confined for sufficient time for the sequential ionization to take place. In a typical ECR ion source, the ion confinement times need to be about 10^{-2} s to produce high charge state ions. The ionization rate depends on the plasma density, which typically ranges from about 10^{11} cm^{-3} for low frequency sources to more that 10^{12} cm^{-3} for the highest frequency sources. Charge exchange with neutral atoms must be minimized, so operating pressures are typically 10^{-6} Torr or less. The plasma chamber is biased positively so that at extraction the ions can be accelerated out of the plasma and into the beam transport system. While the basic principles of operation of an ECR ion source are straightforward, the details of the plasma physics, atomic physics and electron cyclotron heating on one hand, and the technologies needed to produce the high magnetic fields and high frequency microwave power on the other hand, are not simple and will be described briefly in the following sections.

11.4.1 Electron Impact Ionization

In ECR sources multiply charged ions are created mainly by step-by-step ionization, caused by the successive impact of energetic electrons. Therefore the electron impact ionization cross sections are significant parameters. Semi-empirical formulae, fitted to existing experimental results, have been proposed by Müller and Salzborn [43] and Lotz [44]. Figure 11.4 shows electron impact ionization cross sections for argon ions calculated using the Müller-Salzborn formula. Note that the cross section for ionizing argon from 15+ to 16+ is more than 3 orders of magnitude lower than the cross section for ionizing argon to 1+.

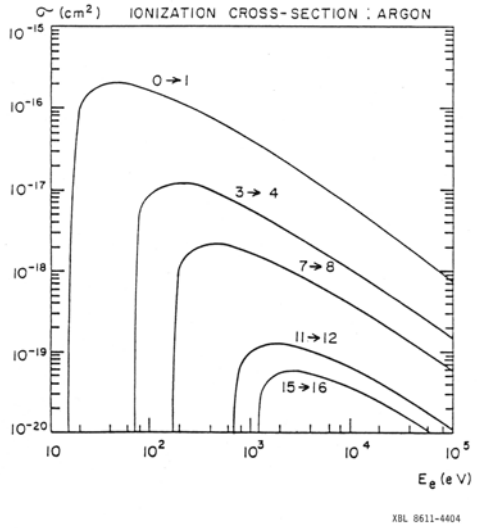

Figure 11.4: Computer calculation of some argon electron impact ionization cross sections using the Müller-Salzborn formula

The rate at which ions of charge state *i* are produced by electron impact ionization of ions with charge state *i-1* is given by

$$R_{prod,i} = n_e \langle \sigma_{i-1,i} v_e \rangle \, n_i \tag{11.1}$$

where n_e is the electron density, $\langle \sigma_{i-1,i} v_e \rangle$, the rate coefficient, is the product of the electron impact ionization cross section from charge *i-1* to *i* and the electron velocity averaged over the electron energy distribution, and n_{i-1} is the density of ions of charge state *i-1*.

11.4.2 Charge Exchange

Two processes dominate the loss of high charge state heavy ions from the plasma. These are charge exchange with neutral atoms in the plasma and loss of confinement. The cross sections for charge exchange between highly charged ions and neutrals are extremely large. An empirical formula, fitting some existing experimental data, has been proposed by Müller and Salzborn [45]. The cross section for charge exchange from initial charge state *i* to final charge state *i-1* is given by

$$\sigma_{i,i-1} = 1.43 \times 10^{-12} \, i^{1.17} \, V_{0,1}^{-2.76} \quad (cm^2) \tag{11.2}$$

where $V_{0,1}$ is the first ionization potential (eV) of the neutral atom. Typical charge exchange cross sections are three to four orders of magnitude larger than corresponding electron impact ionization cross sections. Fortunately, the reaction rates are proportional to the projectile velocities, and neutral atoms are much slower than hot electrons. Still, to keep the rate of production by electron impact equal to the rate of loss by charge exchange for high charge state ions, it is necessary for the neutral atom density in the plasma to be two orders of magnitude lower than the electron density.

11.4.3 Plasma Confinement

The processes that govern particle confinement in an ECR ion source are complex. The temperatures of electrons and ions are different and their confinement times vary considerably. Furthermore, the electron velocity distribution function consists of more than one population, usually described as cold, warm, and hot populations in the literature [46]. Since the confinement times are proportional to the electron temperatures, they are different for each electron population.

The ion confinement time is naturally a very critical parameter in ECR sources. In ECR sources, unlike in other sources like EBIS, it is not possible to arbitrarily interrupt the ion confinement to extract the confined ions. All extracted ions have undergone a loss of confinement – the ion beam is formed from the mirror loss flux. However, if this confinement time is too short, ions do not have time to reach high charge states and if the confinement time is too long, the high charge state ions decay by charge exchange instead of being extracted as a useable beam.

The following short discussion about confinement models in the ECR plasma oversimplifies the processes involved. For a more thorough discussion, we refer to some excellent papers and books [46, 47]. However, most models are based on the assumption of a quiescent plasma and one important conclusion of the available literature is that to improve the confinement of the ECR plasma, turbulence should be avoided. As a result, there is a maximum power density for each ECR source that can be coupled in and a maximum plasma density (typically lower than the cut-off frequency) that can be achieved before plasma instabilities begin to decrease the high charge state performance. These limits increase with frequency and magnetic field strength.

In a simple magnetic mirror structure, particles are confined due to conservation of the magnetic moment μ,

$$\mu = \frac{m v_{\perp}^2}{2B} \tag{11.3}$$

where $v_{\perp}$ is the velocity component transverse to the magnetic field, m is the particle mass and B the magnetic flux density. As the particle moves in the direction of increasing magnetic field strength, its transverse velocity increases so as to satisfy the conservation of magnetic moment. Thus its parallel velocity component, $v_{||}$, decreases according to the conservation of energy. When $v_{||}$ reaches zero the particle is reflected. However, this magnetic confinement is not perfect. If the ratio of the transverse velocity to the parallel velocity is too small the particle will be lost from the plasma. A loss cone can be defined by

$$\sin\theta = \left(\frac{v_{\perp}}{v_{\square}}\right)_{crit} = \sqrt{\frac{B_{\min}}{B_{\max}}} = \sqrt{\frac{1}{R_m}} \tag{11.4}$$

where B_{max} is the peak mirror field, B_{min} is the minimum field, R_m is the mirror ratio, and θ is the loss cone angle (in velocity space) defined by this relationship.

Particles, which oscillate back and forth in the magnetic mirror can be scattered into the loss cone by collisions. Thus the confinement time for ions is related to the scattering rate for ion-ion collisions and the confinement time for electrons is related to the scattering rate for electron-ion collisions. For particles to be magnetically confined, the rate for scattering

through a large angle must be small compared to their gyro frequency in the magnetic field. High energy electrons, which have low collision rates, are well confined. The warm electrons suffer more frequent scattering collisions and are less well confined. On the other hand, the ions are highly collisional and are therefore not magnetically confined [48].

For high charge state ECR ion sources, simple axial mirrors do not provide sufficient magnetic confinement. In addition to the axial magnetic field produced by solenoids, the typical high charge state ECR source uses a sextupole (also called hexapole) or other multipole magnet to produce a radially-increasing field. The combination of the axial mirror field and the radial multipole field produces a "minimum-B" magnetic field configuration, where the magnetic field is a minimum at the center of the device and increases in every direction away from the center. Such a field provides a plasma confinement geometry that is stable against MHD instabilities. The ratio of the maximum field strength at the peak of the magnetic mirrors to the minimum field strength at the center of the device is defined as the axial mirror ratio, $R_m = B_{max}/B_{min}$, as given above. The ratio of the minimum field at the center of the plasma chamber to the maximum field at the plasma chamber wall (moving radially at midplane) defines the radial mirror ratio. While the early ECR ion sources operated with axial and radial mirror ratios with values less than two, the newer sources use mirror ratios as high as 4 at injection, 2 at extraction, and slightly greater than 2 in the radial direction. These higher mirror ratios improve the plasma confinement and this shifts the charge state distribution to a higher average charge.

The minimum-B configuration also makes the ECR heating of the electrons more efficient. Since the electron impact ionization cross sections for high charge state ions is very small, a large flux of high energy electrons is needed to produce a significant density of highly stripped ions. If the electrons travel only once through the system, as in an EBIS (Electron Beam Ion Source), the power flux needed is enormous. For instance, 1 to 10 MW/cm^2 would be required to produce 100 μA of Ar^{8+}. ECR ion sources with a minimum-B structure have excellent plasma confinement properties, thus allowing the electrons to make many passes through the system before they escape from the confinement region, significantly reducing the energy dissipation.

Low energy electrons have poor magnetic confinement and much higher velocities than the ions, which means that their loss rate is higher than the ions. As a result, a positive plasma potential builds up to retard the loss of thermal electrons and enhance the ion loss rate. The positive plasma potential, which has been measured to be 10 to 40 V [49], reduces the ion confinement time and equalizes the global electron and ion losses.

There are several experimental techniques for adding cold electrons to the plasma and thereby lowering the plasma potential, which has several advantages. It reduces the ion loss rate and decreases the voltage gradients in the plasma, which can add to the energy spread and longitudinal emittance of the extracted ion beam. The primary source of cold electrons in these devices is from the stepwise ionization of atoms and ions. However, cold electrons can also be supplied to the plasma from a first stage as used in SUPERMAFIOS and many first generation ECR ion sources, or by enhanced secondary electron emission from the walls [50, 51], or by an electron gun [52], or by a biased disk [53]. A variety of wall coatings have been successfully used to enhance secondary emission including ThO_2 [51], SiO_2 [50], and Al_2O_3 [54], and even special metal-dielectric layers have been tested [55]. Building the plasma chamber from aluminum, which always forms an oxide layer on the surface, is a common method for taking advantage of this effect. Measurements on the AECR showed that the plasma potential could be reduced to about half of its previous value by increasing the supply

of cold electrons from wall coatings or an electron gun [49]. In the most recent ECR ion sources, a negatively biased disk located on axis at the injection end of the plasma chamber is used in place of a first stage or an electron gun. The biased disk reduces the loss of cold electrons at the injection mirror by reflecting those electrons with energies less than the bias voltage. In addition, secondary electrons are generated by ions accelerated into the bias disk. Typical bias disk voltages are 10 to 100 V and the disk currents are from about 1 to 10 mA. For the production of high charge state ions the biased disk voltage is rather critical and should be tuned precisely.

At the core of the plasma the density of hot electrons is high. These hot electrons have a low collision rate and their confinement time is much longer than the lower energy electrons outside of the core. The high density of hot electrons can produce a local negative potential in the center of the trap, retaining high charge state ions and increasing their confinement time [47].

Radially, transverse to the magnetic field, particle losses occur in discrete steps roughly equal to the Lamor radii ρ_i *or* ρ_e. Since the electrons have a much smaller Lamor radius, this diffusion process is mainly important for the ions. The diffusion time is proportional to

$$\tau_D = \tau_{90}\left(\frac{r}{\rho_i}\right)^2 \tag{11.5}$$

where ρ_i is the ion Lamor radius, τ_{90} is the 90° ion scattering time, and r is the plasma radius.

11.4.4 ECR Heating

To optimize the rate of ionization by electron impact, electron temperatures between 1 keV and 20 keV are typically needed. The ion temperature on the other hand should be as low as possible because the ion temperature is one source of emittance and energy spread of the extracted beam. Therefore, a method to selectively heat the electrons in the plasma is desirable. The use of ECRH meets this requirement. If we introduce into the plasma an electromagnetic wave, whose frequency is equal to the cyclotron frequency of the electrons in the magnetic field, an extremely efficient energy transfer occurs between the wave and the electron population. The exact nature of this energy transfer is complex, and has been discussed in numerous papers. A comprehensive discussion has given by Eldridge [56, 57]. In a minimum-B configuration, the magnetic field is not uniform but increases from the center to the outside. Therefore the ECR condition is normally met only on a closed surface around the center, called the "ECR surface". It has been found experimentally that it is essential to have the ECR surface closed inside the plasma chamber. For high performance ECR ion sources, the ECR surface sits well inside of the plasma chamber wall.

The propagation of electromagnetic waves in a plasma is quite complex. In a simplified picture, the plasma can be described as a high-pass filter. Microwaves with frequencies higher than a critical frequency, called the plasma frequency, can propagate while microwaves with frequencies lower than the plasma frequency are reflected. The plasma frequency, f_p, is a function of the plasma density,

$$f_p = \frac{1}{2\pi}\sqrt{\frac{n_e e^2}{\varepsilon_0 m_e}} \tag{11.6}$$

where n_e is the electron density, e is the electron charge, m_e is the electron mass, and ε_0 is the permittivity of free space. For a given microwave frequency, f_{rf}, the critical density, n_{crit} , is defined as the density for which f_p equals f_{rf}. Rewriting equation 11.6 in practical units gives the critical density in terms of the microwave frequency as

$$n_{crit} = 1.26 \times 10^{-8} f_{rf}^2 \tag{11.7}$$

where now n_{crit} is in units of electrons/cm^3 and f_{rf} is the microwave frequency in Hz.

The critical density is an upper bound on the useful plasma density that can be achieved in high charge state ECR ion sources. The production of overdense plasma ($n_e > n_{crit}$) has been demonstrated in some plasma physics experiments using ECRH but the electron temperature remains very low, the ratio of neutral atom density to plasma density is high, and production of high charge state ions is strongly suppressed [58]. Measurements of plasma densities in ECR ion sources have show that the hot electron population makes up roughly 10% of the total electron density, which can be close to the critical density [59]. Therefore, the use of higher frequencies seems the only practical way to reach higher plasma densities in ECR sources. Low frequency ECR ion sources operate at 2.45 GHz where the critical density is 7.6×10^{10} cm^{-3}, many sources now operate at 14.5 GHz or 18 GHz where the critical densities are 2.7×10^{12} and 4.1×10^{12} cm^{-3}, and sources operating at 28 GHz are being developed where the critical density is 9.9×10^{12} cm^{-3}.

11.4.5 Gas Mixing

It was discovered during operation of ECR sources that the production of high charge state ions can be substantially enhanced by adding a light support or mixing gas (typically oxygen) to the ECR plasma [60]. Normally about 80% mixing gas is used and it can be up to 95% or higher for very heavy elements. However, a too high ratio of mixing gas increases the neutral pressure inside the ECR plasma and may also limit the production of higher charge states and the maximum intensity of heavier ions. Gas mixing has been extensively studied both experimentally and theoretically [48]. A widely accepted explanation of this effect is that energy is transferred in collisions between the lighter mixing gas ions and the heavier ions, which cools the heavier ions and increases their confinement time. In addition, the lighter ion also lowers the average charge of the plasma, which again increases the plasma confinement time [47].

11.5 Design Considerations

In this section we will discuss some guidelines for the choice of frequency and magnetic field for high charge state ECR ion sources. Over the last three decades, a wide variety of ECR ion sources have been built and tested. These sources have operated at frequencies that range from 2.45 GHz to 28 GHz. While the axial and radial magnetic mirror ratios in the early sources were modest, in recent years it has become clear that strong confinement fields are important for optimum performance at a given frequency. Early evidence for this came from a series of ECR ion sources called CAPRICE in which the sextupole fields were increased to provide a mirror ratio of at least 2 in both the axial and radial direction [61]. Tests on superconducting ECR ion sources, where the axial and radial fields can be

independently adjusted, have provided further experimental guidelines for optimum magnetic field values [28, 62]. The electron cyclotron resonance magnetic field is given by

$$B_{ecr} = \frac{f}{28} \tag{11.8}$$

where f is the microwave frequency in GHz and B_{ecr} is in Tesla.. The optimum fields can be written as ratios as shown in Table 2.

Table 11.2: Optimum magnetic field ratios for high performance ECR ion sources

B_{inj}/B_{ecr}	~ 4
B_{ext}/B_{ecr}	~ 2
B_{min}/B_{ecr}	~ 0.8
B_{rad}/B_{ecr}	≥ 2
B_{ext}/ B_{rad}	≤ 0.9

where B_{inj} is the maximum axial field strength at the injection end of the plasma chamber, B_{min} is the minimum axial field strength between the mirrors, B_{rad} is the radial field produced by the sextupole at the plasma wall, and B_{ext} is the axial field at extraction.

In addition, to ensure suitable extraction of the beam, the field on axis at extraction should be slightly less than the radial field at the wall. The "optimum" field geometry given in Table 11.2 can be understood in a simple picture where stronger magnetic confinement is provided for the trapped electrons moving either toward injection or radially outward than for those moving toward the extractor. Since the plasma remains neutral up to the plasma meniscus at the extractor, this flow of electrons toward the extraction hole takes the ions with them and enhances the ion density at extraction.

While the dependence of ECR ion source operation on frequency and magnetic field has been well demonstrated, the dependence on the size of the plasma chamber is less clear. At a minimum, the plasma chamber diameter should be at least twice the free space wavelength of the microwave operating frequency so that the plasma chamber acts as a multimode cavity [63]. Recent experiments indicate that in high charge state ECR plasmas the ion confinement times are due to ion diffusion and therefore should depend on the axial length and radial size of the plasma [48].

11.6 Microwave and Magnetic Field Technologies

As described above, the plasma density scales with the square of the microwave frequency and the magnetic field for confinement scale linearly with frequency. The only constraints on using very high frequencies in ECR ion sources are technical and economic. These are related to the generation of high magnetic fields and microwave power at high frequency. Table 11.3 gives the optimum magnetic field values for a range of frequencies used in ECR ion sources. The first generation ECR sources operated at between 6 and 10 GHz and the magnetic fields for these frequencies could be supplied with room temperature copper coils and permanent magnet sextupoles using samarium cobalt. The second generation sources operated at 14 GHz and typically used copper coils with carefully shaped iron yokes to

provide the axial fields and the strongest permanent magnets made with NdFe-B. Another approach is to use permanent magnets to generate both the axial and radial fields. These all permanent magnet ECR ion sources are very compact and have low power consumption [64]. The strongest permanent magnet sextupoles have about 1.4 T at the pole face and due to the thickness of the plasma chamber, the fields at the inner plasma wall are typically reduced to 1.2 T or less. Applying the above guidelines, the optimum fields for 18 and 28 GHz are shown in Table 11.3. Third generation ECR ion sources with frequencies of 18 GHz or greater typically require superconducting magnets to reach the optimum fields although the 18 GHz RIKEN source uses conventional coils and permanent magnets as does PHOENIX which has been tested at 28 GHz. There are also several hybrid ECR ion sources that use superconducting solenoids to produce the axial magnetic field and permanent magnets to produce the radial field [65].

The cost and the complexity of the microwave power also increase with frequency. ECR ion sources can be powered by magnetrons, traveling wave tubes, klystrons, extended wave oscillators, or gyrotrons. For frequencies between 5 and 18 GHz and power levels above 500 W, klystrons are most commonly used. They are commercially available at 6.4, 10, 14 and 18 GHz with CW power capabilities of 2 to 3 kW. In the last few years, laboratory scale gyrotrons have become available that can produce more than 2 kW CW at frequencies above 20 GHz. The SERSE ECR in Catania was tested with a 10 kW 28 GHz gyrotron [62] and the same gyrotron was then used on the Phoenix ECR ion source [66].

Table 11.3: Critical density and optimum fields as function of microwave frequency

Frequency (GHz)	n_{crit} (cm^{-3})	B_{ecr} (T)	B_{inj} (T)	B_{rad} (T)
2.45	7.56 E10	0.088	0.350	0.175
6.45	5.24 E11	0.230	0.921	0.461
10.0	1.26 E12	0.357	1.429	0.714
14.5	2.65 E12	0.518	2.071	1.036
18.0	4.08 E12	0.643	2.571	1.286
28.0	9.88 E12	1.000	4.000	2.000
37.0	1.72 E13	1.321	5.286	2.643

11.7 Metal Ion Beam Production

The diversity of different atomic and nuclear physics experiments performed at facilities around the world requires great variety and flexibility in the production of ion beams. High performance ECR ion sources can provide this flexibility, since they can produce beams of ions as light as hydrogen and as heavy as uranium. Several methods to produce ions from solid materials have been developed over the last twenty years. The most important techniques are: (1) evaporation from external furnaces (ovens), (2) the use of gaseous or volatile chemical compounds, (3) sputtering, (4) direct insertion of solids into the plasma, and (5) evaporation by a laser beam [67]. In some respects all of these techniques are complementary. Figure 11.5 shows charge state distributions for metal ion beam production from various ECR ion sources using all the mentioned techniques [35, 68-72].

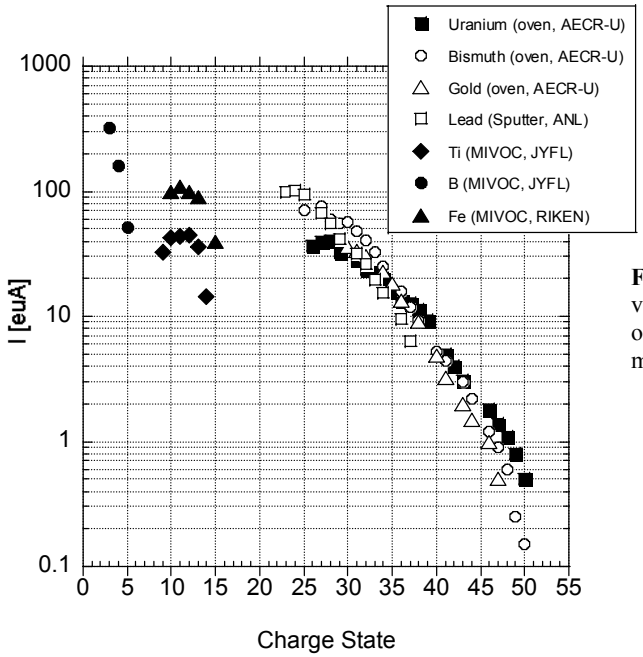

Figure 11.5: Performance of various sources for the production of metal ion beams. The production methods used are also indicated

The selection of the best method to feed solids into ion sources depends on the temperature required to evaporate the metal, the availability of an isotope in a certain chemical form, the intensity, flexibility required, etc. For example, the LBNL ECR and the LBNL AERC-U ion sources are built with radial access. Therefore, several techniques are used simultaneously to provide the maximum flexibility for the production of metal ion beams (see Figure 11.6). The production methods at LBNL include the use of gaseous compounds, the oven technique, the direct insertion method, and the MIVOC method. The following section gives a short overview of the most important techniques.

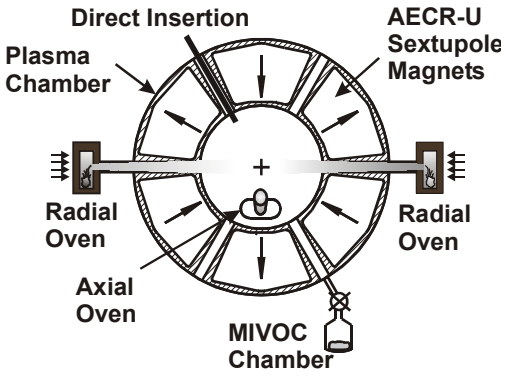

Figure 11.6: Cross section through the AECR-U ion source showing all the different methods used for injection of solid feed

11.7.1 Direct Insertion

The direct insertion technique was one of the first to be utilized for a wide variety of metals [73] and is still used by most ECR groups. A support gas such as oxygen sustains the plasma while a solid rod is positioned close to the plasma, where it is vaporized and the vapor is subsequently ionized. Though the insertion technique is simple and effective, it has the operational disadvantage of strong coupling between plasma and sample heating. However, for some refractory metals (e.g., tantalum) it may be the only choice available. Stable operation can be achieved by carefully controlling the position of the rod.

11.7.2 Sputtering

For the sputtering technique [69, 74], a sample is mounted radially at the periphery of the plasma and is negatively biased with respect to the plasma. The sample is sputtered by the plasma ions, and neutral metal atoms diffuse into the ECR plasma where they are ionized. This technique partly decouples the ECR plasma from the evaporation process. However, adequate plasma density is required to ensure sufficient sputtering rate, and therefore the ion source tuning is not completely decoupled from the evaporation process [70]. Furthermore, the achievable intensities are dependent on the sputtering yield. Thus the sputtering method is very convenient for low intensities, but has limitation for the production of high intensity metal beams.

11.7.3 Gaseous or Volatile Compounds (MIVOC Method)

In some cases, gaseous compounds can be used, especially if the components of the compound can serve as a good mixing gas (see section 11.4.5) Generally, one has to look for compounds with light elements. Sulfur for example can easily be produced from SO_2, CS_2 or H_2S. Oxygen is an excellent mixing gas, therefore a compound containing oxygen is best choice if the desired metal is heavier. If the desired metal is lighter than oxygen, hydrogen is the better choice. Carbon contaminates the plasma chamber walls and should be avoided whenever possible.

The use of volatile compounds was pioneered by Koivisto and Arje [75]. Typically, metallocene materials are used for this method. The metallic compound is loaded into an external chamber and connected to the source by a leak valve. After the initial pump down of the residual gas in the MIVOC chamber, the compound vapor can be introduced into the source as an ordinary gas (see Figure 11.7, [75]). Very successfully applied MIVOC compounds for high intensity metal ion beams are ferrocene $C_{10}H_{10}Fe$ or m-carborane [[35, 68]. The main advantage is the fast setup time and ease of use, but rare isotopes are often not readily available in the appropriate chemical form. Another major drawback is the impurities (in particular carbon, e.g. ten carbon atoms for one Fe atom), which contaminate the plasma chamber walls. The ion source performance and stability can be compromised, particularly for long duration, high intensity applications.

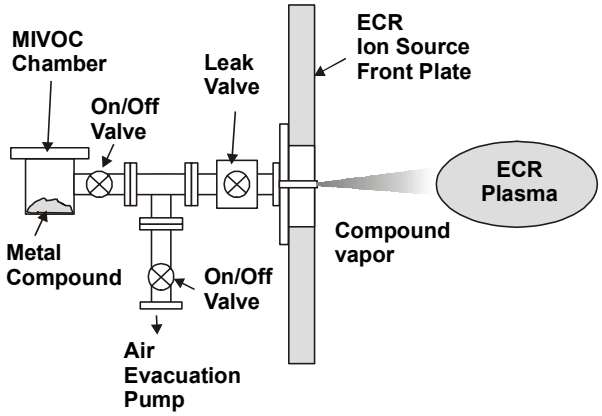

Figure 11.7: Schematic drawing of the MIVOC chamber connected to the plasma stage of an ECR ion source (Courtesy of Hannu Koivisto, JYFL, Finland)

11.7.4 External Furnaces (Ovens)

Of all the methods for the production of metal ion beams, the oven technique is the least intrusive, especially if pure metals can be used. The oven technique was originally developed by Clark and Lyneis at Berkeley [76]. Later the micro-oven concept was developed by the Grenoble group [77] for Caprice type ECR ion sources.

Generally, a metal vapor pressure of about 10^{-3} to 10^{-2} Torr is required inside the oven (for an oven aperture of about 3 mm diameter) to supply the right amount of atomic flux to the ECR plasma. The temperature needed to produce a particular metal ion beam can be estimated from the vapor pressure curve of the metal. Besides the temperature required to evaporate the metal, chemical compatibility of the hot liquid metal and the crucible must be considered [78]. For metals with temperature requirements less than 1600°C ceramic inserts such as zirconia, alumina or yttria can be used to prevent alloying of the heating crucible with the molten metal. For higher temperatures, ceramics begin to sublime and can even react with the hot metals. Therefore, the material has to be either loaded directly into the W or Ta furnace or special crucibles must be used. Chemical compatibility of crucibles for most elements is discussed in reference [78].

If the pure metal is hazardous to handle such as some alkaloids or the isotope is not available as a pure metal, online chemical reactions can be used. For example, alkali metals can be loaded in as alkali chlorides and mixed with calcium. When heated in a low temperature oven CaCl is formed and the pure alkali metal is released into the plasma [79].

If the temperature required is too high, chemical compounds can be utilized to produce the desired metal vapor flux. However, careful consideration should be given when choosing the compound. Oxides, which sublime at lower temperatures, are the best choice for refractory metals since oxygen is an excellent mixing gas. For example, rhenium oxide (Re_2O_7) sublimes sufficiently at temperatures above 140 °C, whereas for the pure metal 2790 °C is needed to reach a vapor pressure of 10^{-3} Torr. Fluorides and chlorides typically also have relatively low working points. However, fluorine and chlorine contaminate the plasma chamber walls and should be avoided.

LBNL [71, 76] and GSI [80] have developed high temperature furnaces that are capable of temperatures up to 2100 ^{o}C. As an example, Figure 11.8 shows the LBNL high temperature oven developed for VENUS, consisting of a resistively heated Ta or W furnace.

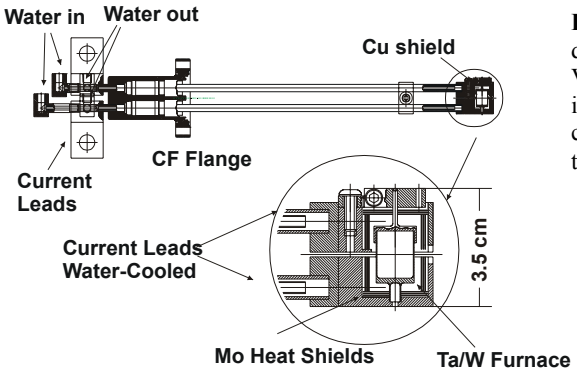

Figure 11.8: High temperature oven designed to be inserted axially into the VENUS ECR ion source. The Ta/W crucible is heated by electric current carried by water-cooled leads. The maximum operating temperature is 2100 ^{o}C

11.7.5 Efficiencies

High efficiency production of high intensity heavy ion beams are desired for various reasons. Firstly, rare isotopes like ^{48}Ca, ^{36}S, and ^{85}Rb are very expensive. Secondly, reloading the oven during long experiments requires several hours of accelerator downtime. Third, it is desirable to minimize the contamination of the ion source over consecutive runs.

At LBNL typical consumption rates for the radial ovens are from 100 to 200 μg/hr.μA, and for the axial oven typical consumption rates are 10 to 40 μg/hr.μA. As shown by the Dubna group [81], a hot tantalum liner covering the plasma chamber walls can be very effective in increasing the overall ion source efficiency. This technique was also tested at Berkeley [71]. The liner, which is heated by the plasma loss flux and by the microwave power, minimizes the condensation of metal vapor on the chamber wall. At a microwave power of 300 W the liner reached a temperature of 400 ^{o}C, corresponding to a vapor pressure of 10^{-4} Torr for Ca. Typical consumption rates of 5 to 10 μg/hr.μA for this setup were measured for ^{48}Ca. The main disadvantage of this method is that the peak charge state for a given metal will shift to lower charge state (for example from 11+ to 9+ for ^{48}Ca) and there is no independent control of the liner temperature. To extend this method for high temperature metals an external heated liner would be necessary.

11.8 Ion Beam Extraction from ECR Ion Sources

Traditionally ECR ion source extraction and analysis systems have been designed for low current, low space-charge ion beams. However, with the dramatic increase in performance over the last decade, modern sources can produce tens of mA of heavy ions, and the extracted ion beams are highly space-charge dominated. Therefore, the beam transport has to be designed as a high current injector system [82]. However, the design is yet more challenging since the ECR ion source produces a spectrum of ions. Consequently, the analyzing system has to have a mass resolution of $m/\Delta m$ of 100 or better to separate the high charge state ions. A typical setup for the analyzing section consists of a combination of a double focusing magnet and one or two solenoid lenses.

Simulation of the extraction and beam transport from the ECR ion source plasmas is complicated by several reasons. First, there are multiple ion charge states present in the plasma (charge state distributions of several ion species), which are all extracted together. Typically, 8 to 30 different ions need to be taken into account to simulate the extraction system for a heavy ion beam. Secondly, the ions are extracted from a strong magnetic field, which as we will show is the dominant cause of beam emittance for ECR ion sources. Third, plasma physics effects also play an important role in the ion source extraction, which are not included in the traditional ECR ion source optics codes. Finally, the ion beam density distribution across the plasma extraction aperture may not be uniform and probably varies for different charge states, which further complicates simulation efforts. In the following section we briefly describe these phenomena.

11.8.1 Influence of Magnetic Field and Ion Temperature on the Extracted Ion Beam Emittance

Ion beam formation from a plasma is described in detail elsewhere in this book. Here we describe phenomena specific to ECR ion sources. For an ECR extraction system two main contributions to the ion beam emittance have to be considered: (1) the ion beam temperature, and (2) the induced beam rotation due to the decreasing axial magnetic field [82].

The emittance due to ion temperature can be estimated by assuming a Maxwellian temperature distribution inside the plasma [83]:

$$\varepsilon_{TEMP}^{xx'-rms-norm} = 0.016\, r \sqrt{\frac{kT_i}{M/Q}} \tag{11.9}$$

where ε is the normalized x-x' rms emittance in π mm.mrad, r is the plasma outlet hole radius in mm, kT_i is the ion temperature in eV, and M/Q is the ratio of ion mass in amu to ion charge state and is dimensionless.

Assuming an uniform plasma density distribution across the plasma outlet hole, the emittance due to beam rotation induced by the decreasing magnetic field in the vicinity of the extractor can be described by Busch's theorem ([84], assuming $\varepsilon^{100\%} = 5 \cdot \varepsilon^{rms}$, a waterbag distribution)

$$\varepsilon_{MAG}^{xx'-rms-norm} = 0.032\, r^2 B_0 \frac{1}{M/Q} \tag{11.10}$$

where ε is the normalized x-x' rms emittance in π mm.mrad, r is the plasma outlet hole radius in mm, B_0 is the axial magnetic field strength at the extractor in T, and M/Q is the ratio of ion mass in amu to ion charge state and is dimensionless.

Beam rotation due to the decreasing magnetic field becomes the dominating contribution to the ion beam emittance when the following condition, derived by combining equations (11.9) and (11.10), is satisfied:

$$B_0 r \geq 0.5 \sqrt{kT_i} \sqrt{M/Q} \tag{11.11}$$

where B_0 is in T, r is in mm, kT_i in eV, and M/Q is dimensionless.

Table 11.4 summarizes the minimum magnetic field values for which the emittance starts to be dominated by the ion beam rotation. A plasma outlet hole radius of 4 mm and an ion temperature of 0.3 eV has been assumed. It is evident that the magnetic field is the main contribution to the ion beam emittance in most ECR ion sources [82].

Table 11.4: Magnetic field for which emittance starts to be dominated by ion beam rotation

M/Q	B_0 (T)
1	0.07 T
5	0.15 T
10	0.22 T
30	0.38 T

As an example the beam rotation in the strong axial magnetic field of the superconducting ECR ion source VENUS is shown in Figure 11.9 for an argon ion beam. Different charge states have different focal lengths and emittance orientations in phase space [85].

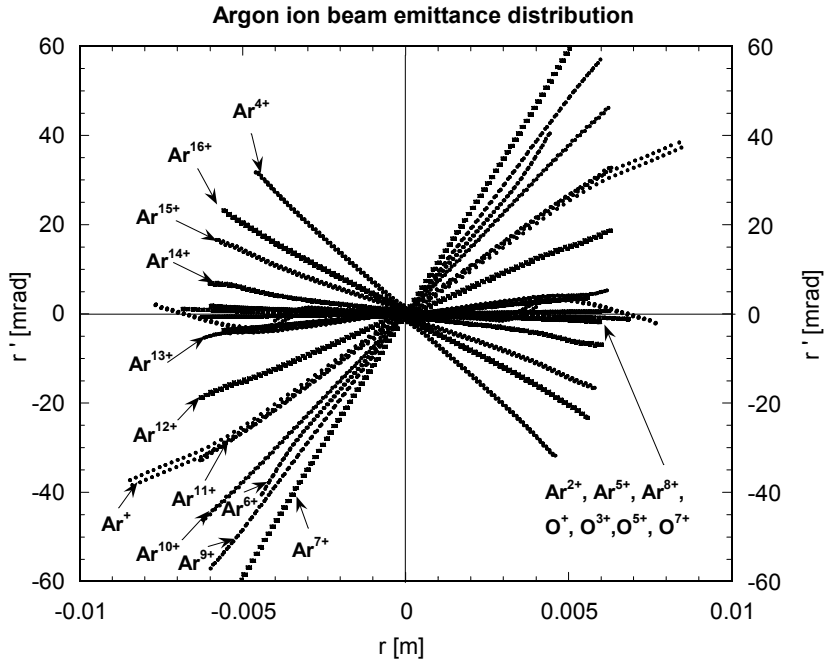

Figure 11.9: Emittance pattern as calculated with AXCEL [85, 86] for a CSD distribution optimized on Ar^{16} with oxygen used as mixing gas.

11.8.2 Influence of Plasma Confinement on Beam Emittance

In addition to the magnetic field at the extractor, the ion confinement in the plasma and plasma stability also play important roles in determining the ion beam emittance.

Experimentally it has been found that, within the charge state distribution for a particular element, the measured emittance decreases for higher charge states [87, 88]. As an example, the dependence of the normalized xx' and yy' emittance values on charge state is shown in detail in Figure 11.10 for a bismuth ion beam extracted from the AECR-U ion source, which was optimized for medium charge state ion production. The beam currents measured for each charge are plotted in Figure 11.11 for reference.

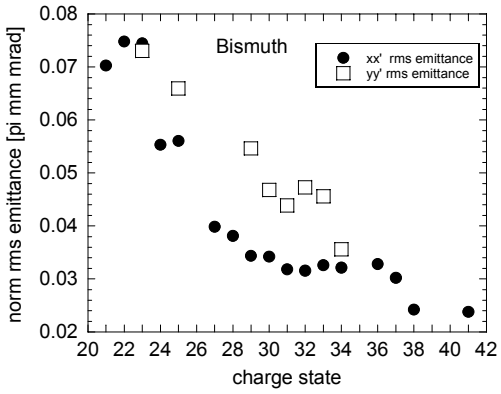

Figure 11.10: Dependence of the normalized xx' and yy' emittances on the charge state for a bismuth ion beam, measured on the AECR-U

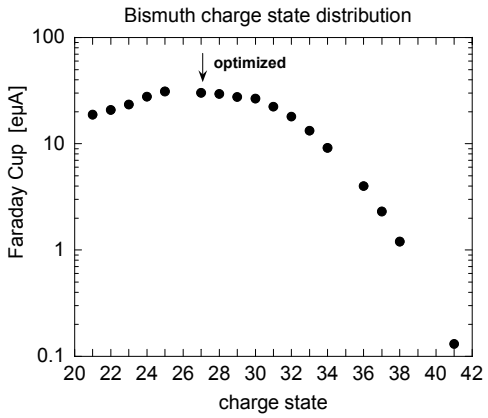

Figure 11.11: Bismuth charge state distribution for the emittance measurements of Figure 11.10

Clearly the emittance value is predominantly dependent on the charge state and not on the current at these ion beam intensities. For instance, the ion beam emittance for an 18.8 eμA beam of Bi^{21+} was measured to be 0.07 π mm.mrad, while the emittance for an 18eμA beam of Bi^{32+} was 0.03 π mm.mrad [88].

Figure 11.12 shows emittance values for beams of several ion species having different masses and charge states as measured after the analyzing magnet of the AECR-U injector ion source at the 88-Inch Cyclotron. The total extracted current was approximately equal for all the different masses (1.5 mA), the peak axial magnetic field at the extractor was ~0.9 Tesla,

and the plasma outlet hole radius was 4 mm. Also plotted in this Figure is the theoretical emittance due to magnetic field in the extraction region.

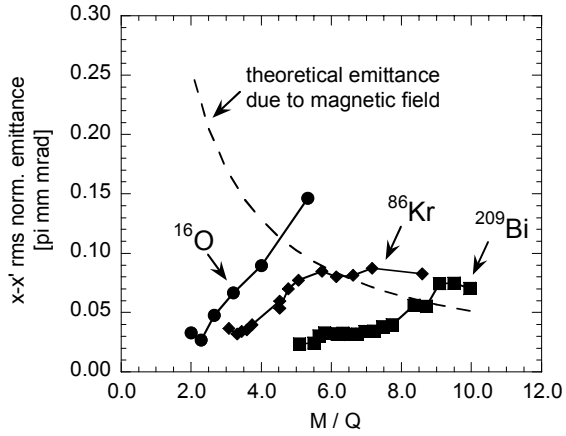

Figure 11.12: Emittance values for various ion masses and charge states as measured after the analyzing magnet of the AECR-U injector ion source at the 88-Inch Cyclotron

The emittance values show a M/Q dependence, which is contrary to the behavior expected from Equation (11.10). The measurements indicate a strong mass dependence of the normalized emittance. For example the normalized rms emittance for O^{3+} (0.146 π mm.mrad) is about 6 times higher than for Bi^{38+} (0.024 π mm.mrad). This behavior cannot be explained by ion optics considerations but must be due to plasma physics and ion production processes, e.g. radial transport phenomena for different ions and electrons. The highly charged heavier ions appear to be concentrated more on the axis of the ion source, whereas the low charge state ions could also be produced in the outer shell of the ECR plasma. Therefore, an effective outlet hole radius may be defined for the higher charge states and heavier masses by comparing the measured emittance values with the theoretical emittance value computed from Equation (11.10)

$$r_{eff} = r_{act}\sqrt{\frac{\varepsilon_{act}}{\varepsilon_{th}}} \tag{11.12}$$

where r_{eff} is the effective extraction aperture (plasma outlet hole) radius; r_{act} is the actual radius; ε_{act} is the measured emittance, and ε_{th} is the theoretical emittance value according to Equation (11.10).

Such effective radii for various ions are plotted in Figure 11.13 for the AECR-U ion beams taken from Figure 11.12. The concentration of high charge state heavy ions on the source axis is clearly visible. The larger extraction radii compared to the actual outlet hole radius for the low charge state ions are most probably caused by beam transport imperfections, e.g. aberrations or unmatched extraction conditions.

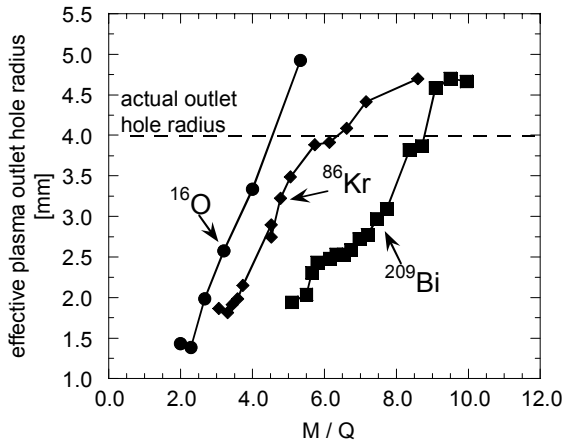

Figure 11.13: Effective extraction radii as defined by equation 11.12 for different ions

The other major factor determining the ion beam emittance is the stability of the plasma. For unstable plasma conditions, the ion beam emittance can easily vary by a factor of 2 or 3 for comparable ion beam intensity [88]. This makes an emittance scanner an extremely useful ion source tuning aid and an important step for understanding the ion beam transport from the source.

11.9 Conclusion

In the 15 years that have elapsed since the first edition of this book was written, there has been remarkable progress in the development of high charge state ECR ion sources. This progress encompasses the major gains in the capability of ECR ion sources to produce intense, high charge state ion beams, and in the development of specialized ECR ion sources for specific applications. In addition, there have been significant improvements in our understanding of the plasma physics of ECR ion sources. We found that fitting this burgeoning field into a single chapter was a major challenge and we were forced to choose between many interesting developments and focus on those that would be most useful to the reader in our view. As a result, some excellent work has gone unmentioned and some areas are only lightly covered. A more detailed description of the plasma physics of ECR sources can be found in Geller's comprehensive book [47] and modeling of ECR plasma has been recently reviewed by Girard et al [89].

In order to produce even more intense, higher charge state beams, higher frequency, higher magnetic field ECR ion sources are being developed. This direction presents major technical and financial challenges. Therefore, the efforts are focused at a few laboratories, which are working to develop a new generation of ECR ion sources for heavy-ion accelerators such as the LHC at CERN [90], RIA in the United States [29, 31] the new heavy ion accelerator storage ring in Lanzhou, HIRFL-CSR [91] and at RIKEN in the future [92]. One of the challenges in the following years will be to find ways to simplify the technology so that very high frequency sources can be applied more widely.

With the development of increasingly powerful ECR ion sources, research has shifted to the better understanding of the transport of the intense, multi species and multi charge ion beam extracted from ECR ion sources. With a better understanding of the ion beam formation at the ECR extraction and the role of the plasma physics on the ion beam emittance, it will be able to further improve the beam quality and intensity from ECR ion sources.

While the most direct path to ECR ion source development is to increase the frequency and magnetic field strengths, it is still possible that other approaches and refinements will lead to significant progress just as it has over the last 15 years. This is especially true in the development of ECR ion sources for special applications such as radioactive ion beams and charge breeders. ECR ion sources remain a fascinating subject for ion source scientists and there is still room for innovation. An especially fruitful effort comes from atomic physics groups at universities, which are developing ECR to conduct basic research and continue to significantly contribute to field [93-97]. One of the great strengths in the field is that young physicists and engineers continue to build new sources, explore new ideas and take on the challenge of developing a new generation of ECR ion sources.

References

[1] V. Bechtold, N. Chan-Tung, S. Dousson, R. Geller, B. Jaquot, and Y. Jongen, Nuclear Instruments and Methods **178**, 305-308 (1980).
[2] D. Hitz, F. Bourg, M. Delaunay, P. Ludwig, G. Melin, M. Pontonnier, and T. M. NGuyen, Rev. Sci. Instrum **67**, 883 (1996).
[3] T. Nakagawa, T. Aihara, Y. Higurashi, M. Kidera, M. Kase, Y. Yano, I. Arai, H. Arai, M. Imanaka, S.M. Lee, G. Arzumanyan, and G. Shirkov, *Rev. Sci. Instrum* to be published (2004).
[4] R. Geller, C. Tamburella, and J. L. Belmont, Rev. Sci. Instrum **67**, 1282 (1996).
[5] P. Sortais, J. F. Bruandet, J. L. Bouly, N. Chauvin, J. C. Curdy, R. Geller, T. Lamy, P. Sole, and J. L. Vieux-Rochaz, Rev. Sci. Instrum **71**, 618 (2000).
[6] T. Lamy, J-F. Bruandet, N. Chauvin, J.-C. Curdy, M. Fruneau, R. Geller, G. Gimond, P. Sole, J-L. Vieux-Rochas, G. Gaubert, L. Maunoury, P. Sortais, and A. C. C. Villari, Rev. Sci. Instrum **69**, 1323 (1998).
[7] J. Sherman, A. Arvin, L. Hansborough, D. Hodgkins, E. Meyer, J.D. Scheider, H.V. Smith Jr., M. Stettler, J. R.R Stevens, M. Thuot, T. Zaugg, and R. Ferdinand, Rev. Sci. Instrum **69**, 1003 (1998).
[8] H. Postma, Phys. Lett **31A**, 196 (1970).
[9] S. Bliman, R. Geller, W. Hess, and B. Jaquot, IEEE Trans. Nucl. Sci. **NS-19**, 200 (1972).
[10] K. Bernhardi and K. Wieseman, Plasma Phys. **14**, 1073 (1972).
[11] R. Bardet, P. Briand, L. Dupas, C. Gormezano, and G. Melin, Nucl. Fusion **15**, 865 (1975).
[12] P. Briand, R. Geller, and B. Jaquot, Nucl. Instrum. Methods **131**, 407 (1975).
[13] Y. Jongen, C. Pirart, G. Ryckewaert, and J. Steyart, IEEE Trans. Nucl. Sci. **NS-26**, 3677 (1979).
[14] V. Bechtold, H.P. Ehret, L. Friedrich, J. Möllenbeck, and H. Schweikert, IEEE Trans. Nucl. Sci. **NS-26**, 3680 (1979).
[15] H. Beuscher, H.G. Mathews, C. Mayer-Börcke, and J. Reich, *Proceedings of the 9th International Conference on Cyclotrons and Their Applications*, (Les Éditions de Physique, Caen, France, 1981).
[16] F. Bourg, R. Geller, B. Jaquot, and M. Pontonnier, *Proceedings of the 4th International Workshop on ECR Ion Sources and Related Topics*, (Centre dÉtudes Nucléaires-Grenoble Press, Grenoble, France, 1982).

[17] V. Bechtold, L. Friedrich, and H. Schweickert, *Proceedings of the 9th International Confererence on Cyclotrons and their Applications*, (Les Éditions de Physique, Caen, France, 1981).
[18] Y. Jongen, C. Pirate, and G. Ryckewaert, *Proceedings of the 4th International Workshop on ECR Ion Sources and Related Topics*, (Centre dÉtudes Nucléaires-Grenoble Press, Grenoble, 1982).
[19] D.J. Clark, J.G. Kalnins, and C. M. Lyneis, IEEE Trans. Nucl. Sci. **NS-30**, 2719 (1983).
[20] F.W. Meyer, *Proceedings of the 6th International Workshop on ECR Ion Sources, Berkeley*, (LBNL, Berkeley, California, 1985).
[21] T.A. Antaya, H.G. Blosser, L.H. Harwood, and F. Marti, *Proceedings of the 6th International Workshop on ECR Ion Sources*, (LBNL, Berkeley, California, 1985).
[22] R. Pardo, E. Minehara, F. Lynch, B. Billquist, W. Evans, B. E. Clift, and M. Waterson, *Proceedings of the 7th International Workshop on ECR Ion Sources*, (KFA-Jülich, Jülich, Germany, 1986).
[23] R. Geller, *Proceedings of the 11th International Conference on Cyclotrons and Their Applications*, (Ionics Publishing Co., Tokyo, Japan, 1986).
[24] Y. Jongen and G. Ryckewaert, IEEE Trans. Nucl. Sci. **NS-30**, 2685 (1983).
[25] H. Beuscher, W. Krauss-Vogt, W. Bräutigam, J. Reich, and P. Wucher, *Proceedings of the 11th International Conference on Cyclotrons and Their Applications*, (Ionics Publishing Co., Tokyo, 1986).
[26] T.A. Antaya and S. Gammino, RSI **65**, 1723-1727 (1994).
[27] D. Hitz, G. Melin, and A. Girad, Rev. Sci. Instrum **71**, 839 (2000).
[28] S. Gammino and C. Ciavola, Rev. Sci. Instrum **71**, 631-636 (2000).
[29] M.A. Leitner, C.M. Lyneis, D.C. Wutte, C.E. Taylor, and S. R. Abbott, Physica Scripta **T92**, 171-173 (2001).
[30] H. W. Zhao, X. Z. Zhang, Z. M. Zhang, X. H. Guo, P. Yuan, Y. Cao, L. T. Sun, B. W. Wei, Y. F. Wang, W. L. Zhan, and D. Z. Xie, Rev. Sci. Instrum **73**, 525 (2002).
[31] C.M. Lyneis, D. Leitner, S.R. Abbott, R.D. Dwinell, M. Leitner, C. Silver, and C. E. Taylor, *Rev. Sci. Instrum* to be published (2004).
[32] Z. Q. Xie, Rev. Sci. Instrum **69**, 625 (1998).
[33] S. Gammino, G. Ciavola, L. Celona, D. Hitz, A. Girad, and G. Melin, Rev. Sci. Instrum **72**, 4090 (2001).
[34] M. Schlapp, R. C. Pardo, R. C. Vondrasek, J. Szczech, P. J. Billquist, J. Vieregg, Z. Q. Xie, C. M. Lyneis, and R. Harkewicz, Rev. Sci. Instrum **69**, 631 (1998).
[35] H. Koivisto, P. Heikkinen, V. Hänninen, A. Lassila, H. Leinonen, V. Nieminen, J. Pakarinen, K. Ranttila, J. Arje, and E. Liukkonen, Nucl. Instrum. Methods B **174**, 379 (2001).
[36] H. Koivisto, J. DeKamp, and A. Zelle, Nucl. Instrum. Methods B **174**, 373 (2001).
[37] S. Gammino, G. Ciavola, L. Celona, M. Castro, F. Chines, and S. Marletta, Rev. Sci. Instrum. **70**, 3577 (1999).
[38] D. Hitz, A. Girard, and G. Melin, *Rev. Sci. Instrum* to be published (2004).
[39] H. Arai, G. Arzumanyan, Y. Higurashi, M. Imanaka, M. Kidera, M. Kase, T. Nakagawa, G. Shirkov, and Y. Yano, *Rev. Sci. Instrum* to be published (2004).
[40] D. Leitner, S. R. Abbott, R. D. Dwinell, M. Leitner, C. Taylor, and C. M. Lyneis, *Proceedings of the Particle Accelerator Conference (PAC'03)*, (The American Physical Society, IEEE, Portland, Or, 2003).
[41] C. E. Taylor, S.R. Abbott, D. Leitner, M. Leitner, and C. M. Lyneis, Advances in Cryogenic Engineering **49 and 50**, (2003).
[42] C. E. Taylor, S. Caspi, M. Leitner, S. Lundgren, C. Lyneis, D. Wutte, S.T. Wang, and J. Y. Chen, IEEE Transactions on Applied Superconductivity **10**, 224 (2000).
[43] A. Müller, E. Salzborn, R. Frodi, R. Becker, H. Klein, and H. Winter, J. Phys. **B 13**, 1877 (1980).
[44] W. Lotz, Z. Phys **216**, 241 (1968).
[45] A. Müller and E. Salzborn, Phys. Lett. **62A**, 391 (1977).
[46] D. Hitz, G. Melin, and A. Girad, Rev. Sci. Instrum **71**, 839 (2000).
[47] R. Geller, *Electron Cyclotron Resonance Ion Source and ECR Plasmas* (Institute for Physics Publishing, Bristol, 1996).

[48] A.G. Drentje, A. Girard, D. Hitz, and G. Melin, Rev. Sci. Instrum **71**, 623 (2000).
[49] Z.Q. Xie and C. M. Lyneis, Rev. Sci. Instrum **65**, 2947-2952 (1994).
[50] C. M. Lyneis, *Proceedings of the International Conference of ECR ion sources and their applications*, (Michigan State University, East Lansing, Michigan, 1987).
[51] R. Geller, F. Bourg, P. Briand, J. Debernardi, M. Delaunay, B. Jaquot, P. Ludwig, R. Pauthenet, M. Pontonnier, and P. Sortais, *Proceedings of the International conference on ECR ion sourcews and their applications*, (MSU, East Lansing, Michigan, 1987).
[52] Z.Q. Xie, C.M. Lyneis, R.S. Lam, and S. A. Lundgren, *Rev. Sci. Instrum* **62**, 775-778 (1990).
[53] G. Melin, C. Barué, F. Bourg, P. Briand, J. Debernardi, M. Delaunay, R. Geller, A. Girard, K.S. Golanovanisky, D. Hitz, B. Jaquot, P. Ludwig, J.M. Mathonnet, T.K. Nguyen, L. Pin, M. Pontonnier, J.C. Rocco, and F. Zadworny, *Proceedings of the 10th International Workshop on ECR ion sources*, (ORNL, Knoxville, Tennessee, 1990).
[54] T. Nakagawa, Japanese Journal of Applied Physics **30**, 930 (1991).
[55] L. Schachter, S. Dobrescu, K. E. Stiebing, and J. D. Meyer, *Rev. Sci. Instrum* to be published (2004).
[56] O. Eldridge, Phys. Fluids **15**, 676 (1972).
[57] A. Girard, D. Hitz, G. Melin, and K. Serebrennikov, *Rev. Sci. Instrum* to be published (2004).
[58] K. Golovanivsky, *Proceedings of the 12th International Workshop on ECR ion sources*, (Institute for Nuclear Study, University of Tokyo, RIKEN, Japan, 1995).
[59] A. Girard, P. Briand, G. Gaudart, J.P. Klein, F. Bourg, J. Debernardi, J.M. Mathonnet, G. Melin, and Y. Su, Rev. Sci. Instrum **65**, 1714-1717 (1994).
[60] H. Beuscher, W. Krauss-Vogt, and H. G. Mathews, *Proceedings of the 5th International Workshop on ECR ion sources*, (LBNL, Berkeley, California, 1985).
[61] B. Jaquot and M. Pontonnier, *Proceedings of the 10th International ECR ion source conference*, (ORNL, Knoxville, Tennessee, 1990).
[62] D. Hitz, A. Girard, G. Melin, S. Gammino, G. Ciavola, and L. Celona, Rev. Sci. Instrum **73**, 509-512 (2002).
[63] C. M. Lyneis, *Proceedings of the 1987 IEEE Particle Accelerator Conference*, (IEEE, Washington DC, 1987).
[64] P. Sortais, J. Debernardi, R. Geller, P. Ludwig, and R. Pauthenet, *Proceedings of the International conference on ECR ion sources and their applications*, (MSU, East Lansing Michigan, 1987).
[65] T Nakagawa, T. Kurita, M. Imanaka, Y. Higurashi, M. Tsukada, S. M. Lee, M. Kase, and Y. Yano, Rev. Sci. Instrum **73**, 513-515 (2002).
[66] T. Thuillier, J.L Bouly, J.C. Curdy, T. Lamy, C. Peaucelle, P. Sole, P. Sortais, J.L. Vieux-Rochaz, and D. Voulot, *Proceedings of the 15th International Workshop on ECR ion sources, ECRIS'02*, (JYFL, Jväskylä, Finland, 2002).
[67] R. Harkewicz, Rev. Sci. Instrum **66**, 2883 (1995).
[68] T. Nakagawa, J. Ärje, Y. Miyazawa, M. Hemmi, T. Chiba, N. Inabe, M. Kase, T. Kageyama, O. Kamigaito, M. Kidera, A. Goto, and Y. Yano, Rev. Sci. Instrum **69**, 637 (1998).
[69] R. C. Vondrasek, R. Scott, and R. C. Pardo, *Rev. Sci. Instrum* to be published (2004).
[70] R. C. Vondrasek, private communications, (Argone National Laboratory, 2003).
[71] D. Wutte, S. Abbott, M. Leitner, and C. M. Lyneis, Rev. Sci. Instrum **73**, 521 (2002).
[72] H. Koivisto, J. Ärje, R. Seppälä, and M. Nurmia, Nucl. Instrum. Methods B **187**, 111 (2002).
[73] F. Bourg, R. Geller, and B. Jacquot, Nucl. Instrum. Methods A **254**, 13 (1987).
[74] D. P. May, Rev. Sci. Instrum **69**, 688 (1998).
[75] H. Koivisto, J. Arje, and M. Nurmia, Rev. Sci. Instrum **69**, 785 (1998).
[76] D. J. Clark and C. M. Lyneis, Journal de Physique **50**, C1-759 (1989).
[77] G. Melin, F. Bourg, P. Briand, M. Delaunay, G. Gaudart, A. Girard, D. Hitz, J. P. Klein, P. Ludwig, T. K. Nguyen, M. Pontonnier, and Y. Su, Rev. Sci. Instrum **65**, 1051 (1994).
[78] K. J. Ross and B. Sonntag, Rev. Sci. Instrum **66**, 4409 (1995).
[79] DeMarco B., Rohner H., and D. S. Jin, Rev. Sci. Instrum **70**, 1967 (1999).

[80] R. Lang, J. Bossler, R. Iannucci, and K. Tinschert, *Proceedings of the ECR Workshop 2002*, (University of Jyvaskyla, Jyvaskyla, Finnland, 2002).
[81] V. Kutner, S. L. Bogomolov, A. A. Efremov, A. N. Lebedev, V. N. Loginov, A. B. Yakushev, and N. Y. Yazivitsky, Rev. Sci. Instrum **70**, 860 (2000).
[82] M. A. Leitner, D. C. Wutte, and C. M. Lyneis, *Proceedings of the Particle Accelerator Conference (PAC'01)*, (The American Physical Society, IEEE, Chicago, 2001).
[83] I. A. Brown, *The Physics and Technology of Ion Sources* (Wiley-Interscience Publication, New York, 1989).
[84] A. Septier, *Focusing of charged particles* vol. 2 (Academic Press,, New York, 1967).
[85] D. Wutte, M. Leitner, C. M. Lyneis, C. E. Taylor, and Z. Q. Xie, *Proceedings of the Heavy Ion Accelerator Technology Conference (HIAT'98), AIP Conference Proceedings*, (American Institute of Physics, Argonne National Laboratory, Illinois, 1998).
[86] P. Spaetke, *ACXEL*, ion optics simulation program, (INP, Junkernstr. 99, 65205 Wiesbaden, Germany; http://www.inp-dme.com/)
[87] P. Sortais, L. Maunoury, A. C. Villari, R. Leroy, J. Mandin, J. Y. Pacquet, and E. Robert, *Proceedings of the Proceedings of the 13th International Workshop on ECR Ion Sources*, (Texas A&M University, College Station, Texas A&M University, 1997).
[88] D. Wutte, M. Leitner, and C. M. Lyneis, Physica Scripta **T92**, 247 (2001).
[89] A. Girard, K. Serebrennikov, G. Melin, R. Vallcorba, and C. Lécot, Rev. Sci. Instrum **73**, 1146 (2002).
[90] S. Gammino, G. Ciavola, L. Celona, L. Andó, M. Menna, L. Torrisi, D. Hitz, A. Girard, P. Seyfert, and D. Guillame, *Proceedings of the 15th International Workshop on ECR Ion Sources*, (JYFL, Jyväskylä, Finland, 2002).
[91] H.W. Zhao, Z.M. Ahang, W. He, X.Z. Zhang, X.H. Guo, Y. Cao, P. Yuan, L.T. Sun, L. Ma, M.T. Song, W.L. Zhan, B.W. Wei, and D. Z. Xie, *Rev. Sci. Instrum* to be published (2004).
[92] T. Nakagawa, T. Kurita, M. Imanaka, H. Arai, M. Kidera, Y. Higurashi, S.M. Lee, M. Kase, and Y. Yano, *Proceedings of the 15th International Workshop on ECR Ion Sources*, (JYFL, Jyväskylä, Finland, 2002).
[93] V. Mironov, K. E. Stiebing, O. Hohn, L. Schmidt, H. Schmidt-Böcking, S. Runkel, A. Schempp, G. Shirkov, S. Biri, and L. Kenéz, Rev. Sci. Instrum **73**, 623 (2002).
[94] P. Grübling, J. Hollandt, and G. Ulm, Rev. Sci. Instrum **73**, 614 (2002).
[95] M. Leitner, D. Wutte, J. Brandstötter, F. Aumayr, and H. Winter, Rev. Sci. Instrum **65**, 1091 (1994).
[96] L. Muller, A. Heinen, H. W. Ortjohann, and H. J. Andra, Rev. Sci. Instrum **73**, 1140 (2002).
[97] A. Heinen, M. Rüther, J. Ducrée, J. Leuker, J. Mrogenda, H. W. Ortjohann, E. Reckels, Ch. Vitt, and H. J. Andrä, Rev. Sci. Instrum. **69**, 729 (1998).